



A simple fluorescent probe for Zn(II) based on the aggregation-induced emission

De-Xun Xie^a, Zhao-Jin Ran^{a,b}, Zhen Jin^a, Xiao-Bing Zhang^{a,*}, De-Lie An^{a,*}

^a State Key Laboratory for Chemo/Biosensing and Chemometrics, College of Chemistry and Chemical Engineering, Hunan University, Changsha 410082, PR China

^b College of Sciences, China Agricultural University, Beijing 100193, PR China

ARTICLE INFO

Article history:

Received 5 September 2012

Received in revised form

7 October 2012

Accepted 8 October 2012

Available online 17 October 2012

Keywords:

Fluorescent probe

Salicylaldehyde

Hydrazine

Zn²⁺ detection

Red shift

Aggregation-induced emission (AIE)

ABSTRACT

A aggregation-induced emission-based fluorescent probe **1** for Zn²⁺ was designed and simply synthesized by condensation of salicylaldehyde with aqueous hydrazine. The experimental conditions were first optimized. It was found that N, N-Dimethylformamide (DMF) was the best solvent for the Zn²⁺-triggered aggregation of compound **1** compared with other solvents. The emission intensity was gradually increased, accompanied by the simultaneous red shift of the maximum emission peak with increasing Zn²⁺ concentrations. A red shift about 45 nm was achieved when Zn²⁺ concentration is 100 μM. Compared with other Zn²⁺ fluorescent sensors based on aggregation-induced emission (AIE), compound **1** can detect a lower concentration of Zn²⁺ with a detection limit of 0.1 μM. Compound **1** also exhibited good selectivity toward Zn²⁺. The aggregation was verified by the dynamic light scattering (DLS) results, with a Zn²⁺ concentration-dependent size observed. It was also directly confirmed by TEM analyses.

© 2012 Elsevier Ltd. All rights reserved.

1. Introduction

Following iron, zinc ranks the second in abundance among the transition metals in the human body, and plays vital roles in many biological processes such as cellular metabolism, gene expression, and immune function [1–3]. Zn²⁺ is also believed to be an essential factor in some pathological processes, including Alzheimer's disease, epilepsy, and ischemic stroke [4,5]. Therefore, it is important to monitor Zn²⁺ in many scientific fields and clinical situations.

In the past few years, many traditional analytical techniques such as atomic absorption spectrometry [6], flame atomic absorption spectroscopy [7], inductively coupled plasma–atomic emission spectrometry [8], mass spectrometry [9], and cyclic voltammetry methods [10] have been employed to detect the concentration of Zn²⁺. Though these techniques are sensitive, selective, and accurate for Zn²⁺ detection, most of them are rather complicated, time-consuming, and expensive as well as inadequate for on-line monitoring. Owing to the advantages of simplicity and inexpensive instrumentation, there are many methods such as spectrophotometric and fluorophotometric methods reported for the determination of trace amounts of zinc. Up to now, a variety of Zn²⁺-selective fluorescent probes have been reported, most of

which are based on photoinduced electron transfer (PET) [11–14], internal charge transfer (ICT) [13,15–17], and fluorescence resonance energy transfer (FRET) [18–22]. In recent years, various aggregation-induced emission (AIE) active compounds have been synthesized [23,24,27], and several Zn²⁺-selective fluorescent turn-on probes based on aggregation-induced emission have also been developed [24,25].

Although the synthesis and optical property of 1,2-bis(2-hydroxybenzylidene) hydrazine have been previously reported [26], its analytical recognition characteristics are not investigated up to date. It was found that it is practically nonluminescent in the solution state, but becomes highly emissive as nanoparticle suspensions in poor solvents, demonstrating a novel phenomenon of AIE [27]. By taking advantage of the AIE feature of 1,2-bis(2-hydroxybenzylidene) hydrazine **1** (Scheme 1), herein we report a new fluorescence turn-on probe **1** for Zn²⁺. Compound **1** exhibited good selectivity and sensitivity toward Zn²⁺.

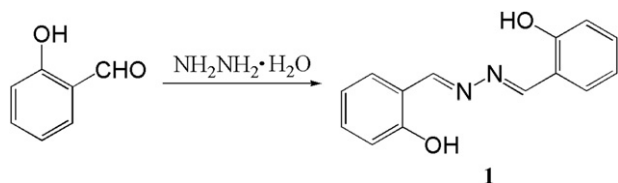
2. Experimental

2.1. General

Chemicals were purchased from commercial suppliers and used without further purification. Double-distilled water was used throughout all experiments. Thin layer chromatography (TLC) was carried out using silica gel HSGF254, which were obtained from the Qingdao Ocean Chemicals (Qingdao, China). NMR spectra were

* Corresponding authors.

E-mail addresses: xbzhang@hnu.edu.cn, xiaobingzhang89@hotmail.com (X.-B. Zhang), deliean@hnu.edu.cn (D.-L. An).



Scheme 1. Synthetic routes of compound 1.

recorded on a Bruker DRX-400 spectrometer operating at 400 MHz. LC-MS analyses were performed using an Agilent 1100 HPLC/MSD spectrometer. All fluorescence measurements were carried out on a Hitachi-F4500 fluorescence spectrometer with excitation slit set at 5 nm and emission at 5 nm. Dynamic light scattering (DLS) characterization was performed using a Zetasizer Nano ZS90 DLS system. The morphology and particle size distribution of particles were characterized using a Jeol JEM-2010 transmission electron microscopy.

2.2. Synthesis of compound 1

Compound 1 was synthesized according to a reported method (Scheme 1) [28]. To a solution of aqueous hydrazine (13 mg, 2.25 mmol) in methanol (20 mL) was added salicylaldehyde (549 mg, 4.50 mol) over a period of 1 h. Then the mixture was refluxed for 4 h. The solution was concentrated to give crude solid, which was recrystallized methanol and dried in vacuo to get 421 mg (78%) of compound 1 as a pale yellow solid. ^1H NMR (400 Hz, CDCl_3): 6.97 (t, $J = 7.2$ Hz, 2H), 7.04 (d, $J = 8.0$ Hz, 2H), 7.35–7.42 (m, 4H), 8.72 (s, 2H), 11.34 (brs, 2H); ^{13}C NMR (100 Hz, CDCl_3): δ 117.16, 119.72, 132.55, 133.44, 159.81, 164.70; ESI-MS: calcd for $\text{C}_{14}\text{H}_{12}\text{N}_2\text{O}_2$ m/z 240.3, found $(\text{M} + \text{H})^+$: 241.1.

2.3. Procedures for metal ion sensing

A 11.11 μM stock solution of 1 was prepared by dissolving 1 in DMF. A standard stock solution of Zn^{2+} (10 mM) was prepared by dissolving an appropriate amount of zinc nitrate in water and

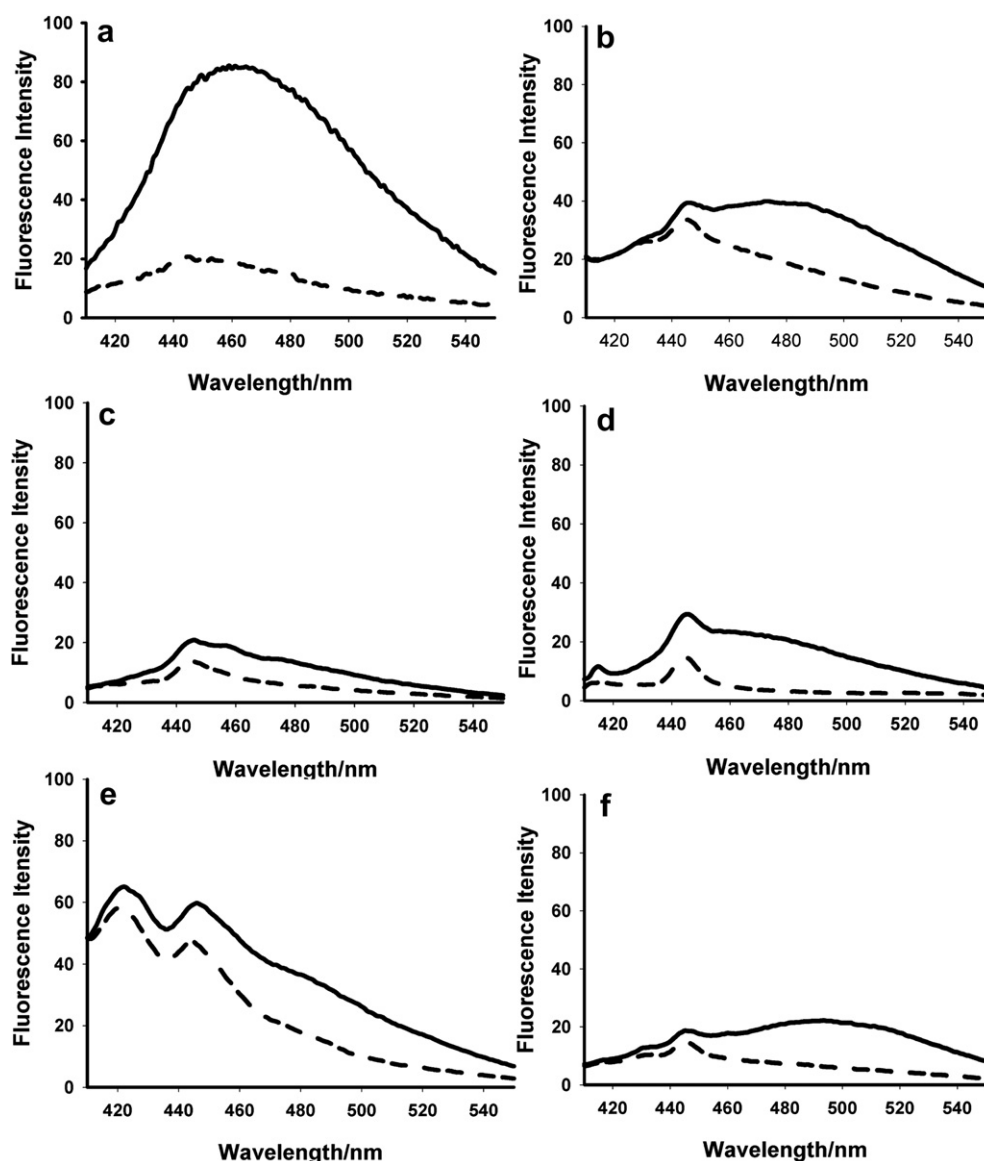


Fig. 1. Fluorescence emission spectra of the fluorescence chemosensor exposed to various solvents (dotted line: compound 1; solid line: compound 1 with Zn^{2+}): a) DMF; b) DMSO; c) CH_3OH ; d) THF; e) $\text{C}_2\text{H}_5\text{OH}$; f) CH_3CN . $\lambda_{\text{ex}} = 400$ nm.

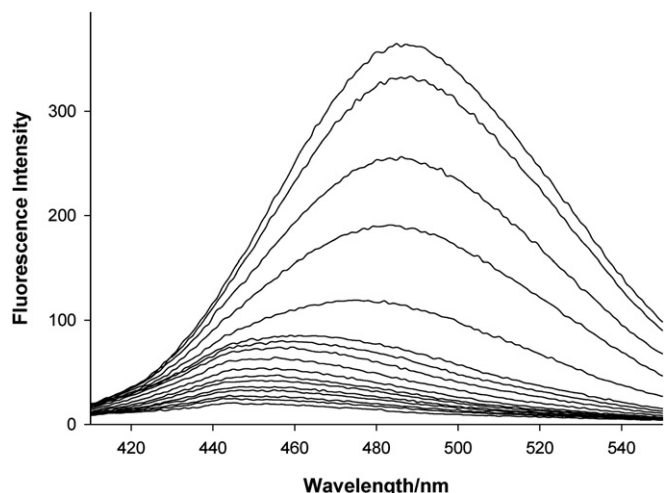


Fig. 2. Fluorescence emission spectra of the fluorescence chemosensor exposed to Zn^{2+} of various concentrations: 0 , 1.0×10^{-7} , 2.0×10^{-7} , 4.0×10^{-7} , 6.0×10^{-7} , 8.0×10^{-7} , 1.0×10^{-6} , 2.0×10^{-6} , 4.0×10^{-6} , 6.0×10^{-6} , 8.0×10^{-6} , 1.0×10^{-5} , 2.0×10^{-5} , 4.0×10^{-5} , 6.0×10^{-5} , 8.0×10^{-5} , 1.0×10^{-4} mol/L from bottom to top. These spectra were measured in water/DMF (1:9, v/v) solution. $\lambda_{\text{ex}} = 400$ nm.

adjusting the volume to 500 mL in a volumetric flask. This was further diluted to 1.0×10^{-3} – 1.0×10^{-6} M stepwise. The complex solution of $\text{Zn}^{2+}/\mathbf{1}$ was prepared by adding 900 μL of the stock solution of $\mathbf{1}$ and 100 μL of the stock solution of Zn^{2+} . In the resultant solution, the concentrations were 10 μM of $\mathbf{1}$ and 0.1 mM–0.1 μM of Zn^{2+} . Blank solution of $\mathbf{1}$ was prepared under the same conditions without Zn^{2+} . Stock solutions of other metal ions were prepared in water with a similar procedure. The fluorescence emission spectra were recorded at an excitation wavelength of 400.0 nm with an emission wavelength range from 410 nm to 550 nm with excitation slit set at 5 nm and emission slit set at 5 nm.

3. Results and discussion

3.1. Sensitivity of compound **1** in different solvents

In order to achieve the best sensitivity of the probe, compound **1** was dissolved in DMF, DMSO, CH_3OH , THF, $\text{C}_2\text{H}_5\text{OH}$, CH_3CN , respectively. As shown in Fig. 1, Compound **1** in DMF showed the

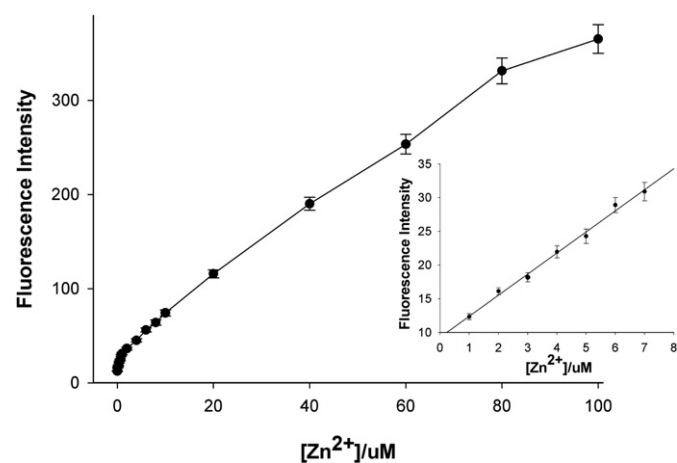


Fig. 3. Fluorescence titration curve of compound **1** with Zn^{2+} in water/DMF (1:9, v/v) solution. Inset shows the fluorescence responses at low Zn^{2+} concentrations. $\lambda_{\text{ex}} = 400$ nm, $\lambda_{\text{em}} = 485$ nm.



Fig. 4. Photographs of **1** in DMF treated with different metal ions at 1.0×10^{-4} M (Cd^{2+} , Co^{2+} , Cr^{3+} , Cu^{2+} , Mn^{2+} , Ni^{2+} , Pb^{2+} , Hg^{2+} , Fe^{2+} , Fe^{3+} and Zn^{2+} , from left to right).

best sensitivity with a wavelength red shift among the chosen water-solubility organic solvents. So we chose DMF as the solvent through our subsequent experiment.

3.2. Analytical performance characteristics of compound **1**

Fig. 2 shows the fluorescence spectra of **1** in water/DMF (1:9, v/v) after mixing with aqueous solutions containing different concentrations of Zn^{2+} . They were recorded with an excitation at 400.0 nm and emission wavelength of 410–550 nm. In the absence of Zn^{2+} , Compound **1** in water/DMF (1:9, v/v) did not emit any obvious and characteristic fluorescence. With the introduction of Zn^{2+} , a new emission band with the maximum emission wavelength at 445 nm appeared. Moreover, the emission intensity was gradually increased with the increasing Zn^{2+} concentration (Fig. 2). Meanwhile, the maximum emission band was red-shifted with increasing Zn^{2+} concentrations, with an emission red shift of 40 nm observed when Zn^{2+} concentration reached 1.0×10^{-4} M. This provides the basis for the detection of Zn^{2+} with fluorescent probe, as used in our following study. A detection limit of 1.0×10^{-7} M (3 times the standard deviation in the blank solution) for Zn^{2+} is established under current experimental conditions, lower than the other Zn^{2+} fluorescent sensors based on tetraphenylethylene with aggregation-induced emission (AIE) [24] (Fig. 3 inset).

3.3. Selectivity of compound **1**

Achieving highly selective response to analytes of interest over other potentially competing species coexisting in the sample is a necessity for a probe with potential application for practical use.

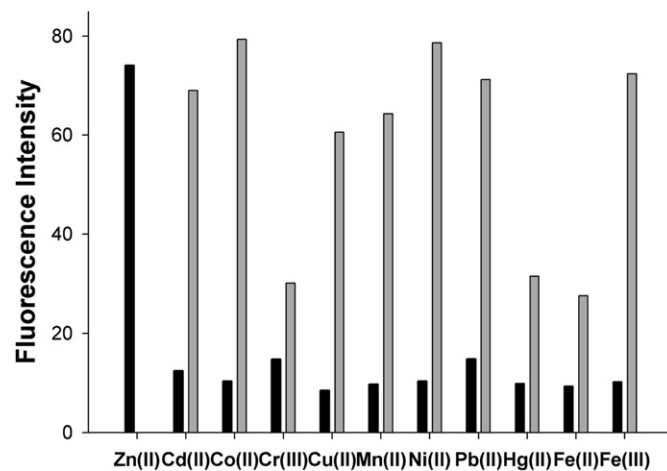


Fig. 5. Fluorescence response of 10 μM **1** to 1.0×10^{-5} M of Zn^{2+} or other metal ions (the black bar portion) and to the mixture of 10 μM of other metal ions with 10 μM of Zn^{2+} (the gray bar portion), $\lambda_{\text{ex}} = 400$ nm, $\lambda_{\text{em}} = 485$ nm.

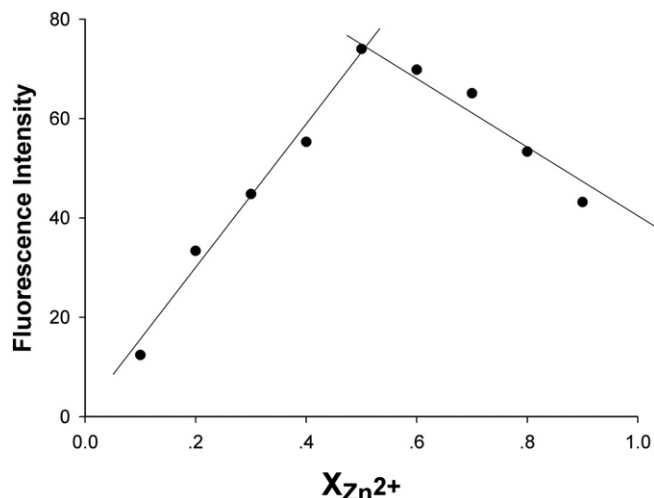


Fig. 6. Job's plot for **1** and Zn^{2+} . The total concentration of **1** and Zn^{2+} kept at 1.0×10^{-5} mol/L. $\lambda_{ex} = 400$ nm, $\lambda_{em} = 485$ nm.

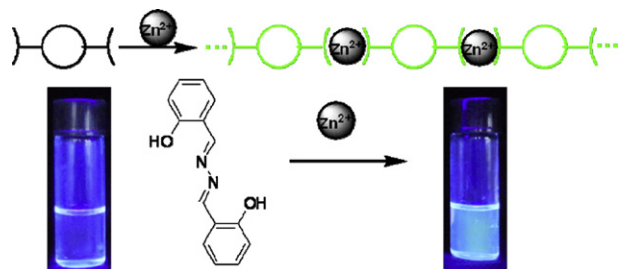
Therefore, the selectivity and competition experiments were extended to a variety of other metal ions, such as common transition metal ions (Co^{2+} , Cu^{2+} , Mn^{2+} , Ni^{2+} , Fe^{2+} and Fe^{3+}), and environmentally relevant heavy metal ions (Cd^{2+} , Pb^{2+} , Cr^{3+} and Hg^{2+}). The compound **1** emitted strong fluorescence near 485 nm ($[Zn^{2+}] = 100 \mu M$, excited at 400 nm) (Fig. 4). However, amongst other heavy metal ions (Cd^{2+} , Cr^{3+} , Co^{2+} , Cu^{2+} , Mn^{2+} , Ni^{2+} , Pb^{2+} , Hg^{2+} , Fe^{2+} and Fe^{3+}) that usually show an interfering effect on Zn^{2+} ion assays, only Cr^{3+} , Hg^{2+} and Fe^{2+} showed fluorescence quenching after they were respectively added to compound **1** (Fig. 5). This clearly indicated that our proposed probe exhibits high selectivity to Zn^{2+} over Cd^{2+} and other competing metal ions.

3.4. The schematic illustration of the coordination modes between **1** and Zn^{2+}

To determine the binding stoichiometry of **1** and Zn^{2+} , Job's method for the emission was employed. The concentrations of **1** and Zn^{2+} were varied, while the sum of the two concentrations kept constant at 1.0×10^{-5} mol/L. The change of the fluorescence intensity at 485 nm with a serial of concentration ratios of **1** to Zn^{2+} is shown in Fig. 6. When the molecular fraction of Zn^{2+} was closed to 50%, the complex of **1** and Zn^{2+} exhibited a maximum fluorescence emission at 485 nm. This indicated that a 1:1 stoichiometry is possible for the binding mode of **1** and Zn^{2+} . The schematic illustration of the coordination modes between **1** and Zn^{2+} was shown in Scheme 2.

3.5. Confirmation the aggregation of compound **1**

These spectrum changes should be attributed to the coordination of Zn^{2+} with N and O groups. Such coordination could inhibit



Scheme 2. Schematic illustration of the coordination modes between **1** and Zn^{2+} .

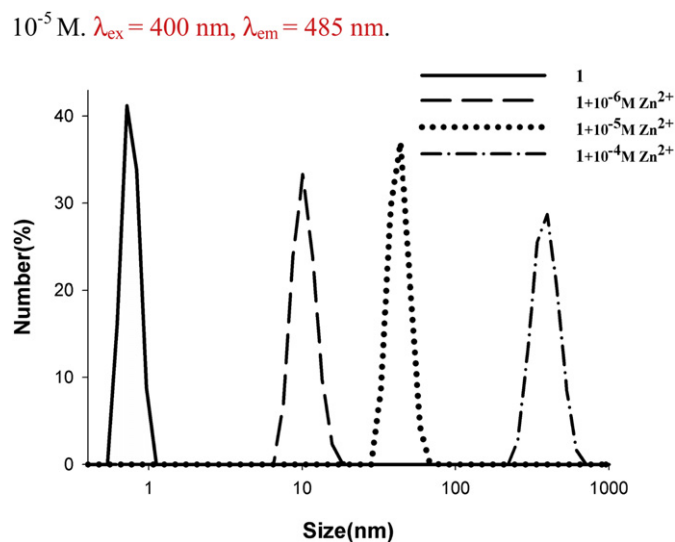


Fig. 7. DLS profiles (from left to right) of **1** ($10 \mu M$ DMF solution) and in the presence of $1 + 10^{-6}$ M Zn^{2+} , $1 + 10^{-5}$ M Zn^{2+} , and $1 + 10^{-4}$ M Zn^{2+} , respectively.

the PET within **1**, but this alone still cannot turn-on the fluorescence of compound **1**. Possible coordination modes of **1** with Zn^{2+} may exist as following (Scheme 2): One Zn^{2+} ion coordinates with two compound **1**, leading to coordination oligomers and even polymers. These coordination oligomers and polymers may exhibit lower solubility in water/DMF solution, and accordingly the fluorescence from **1** will emerge due to AIE. The intermolecular coordination may become dominant at high concentration of Zn^{2+} , which was verified by the dynamic light scattering (DLS) results. As depicted in Fig. 7, the initial DLS signal corresponds to species of

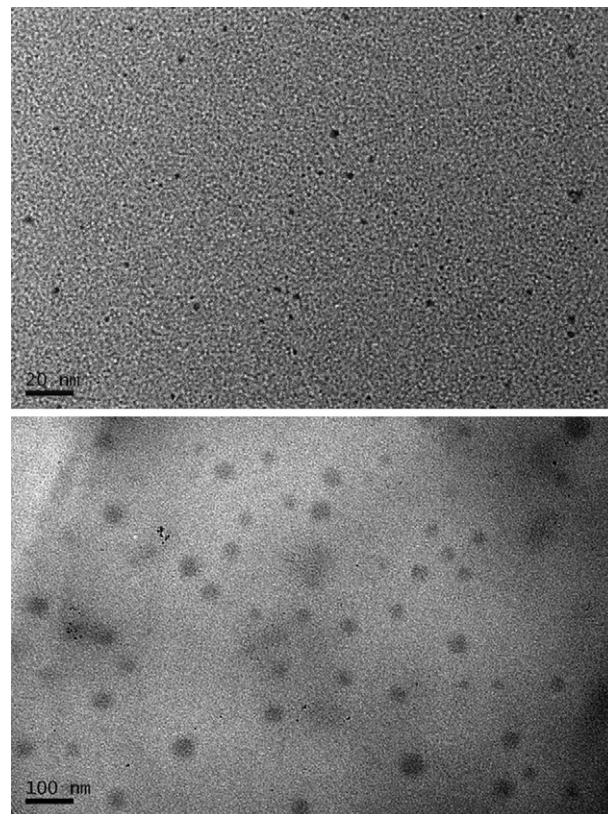


Fig. 8. TEM images of compound **1** ($10 \mu M$) in water/DMF (1:9, v/v) before (upper) and after (lower) addition of 1.0×10^{-5} M Zn^{2+} .

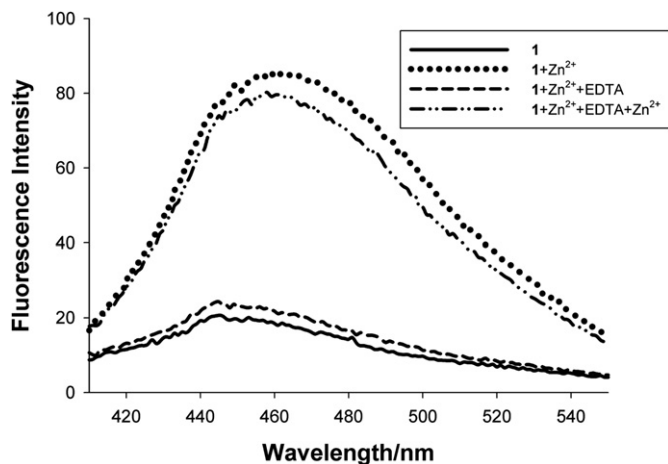


Fig. 9. Reusability of compound **1** toward Zn^{2+} (1.0×10^{-5} M). $\lambda_{\text{ex}} = 400$ nm.

0.7 nm approximately, agreeing well with the molecular size of **1**. This also shows that **1** can be well dissolved and dispersed in DMF solution. However, upon the introduction of $1 \mu\text{M}$ of Zn^{2+} , aggregates with a size of about 10 nm were observed, and the size of aggregates was increased with increasing concentration of Zn^{2+} added. Such an experimental result should be attributed to the aggregation of the coordination oligomers and polymers, and was also directly confirmed by TEM analyses (Fig. 8).

3.6. Reversibility of compound **1**

As well known, the reversibility is an important factor to obtain an excellent chemical sensor. Thus, the chemical reversibility behavior of compound **1** was studied to examine the reusability of the probe **1** (Fig. 9). It is shown clearly that the fluorescence intensities of solution containing **1** and Zn^{2+} decreased with the introduction of EDTA, and when more Zn^{2+} was added to the system afterward, the fluorescence intensities were recovered. The experimental result indicates that the present compound **1** could be easily regenerated for repeated use.

4. Conclusion

A new fluorescent sensor for Zn^{2+} has been developed by taking advantage of the AIE feature of compound **1**. This sensor for Zn^{2+} was unique in terms of the following points: (1) the sensing mechanism was different from most previously reported; (2) Compound **1** was able to be synthesized with relative ease; (3) Compound **1** exhibited high sensitivity and good selectivity toward Zn^{2+} .

Acknowledgments

This work was supported by the National Key Scientific Program of China (2011CB911000), NSFC (Grants 20975034, 21177036), the National Key Natural Science Foundation of China (21135001), National Instrumentation Program (2011YQ030124), the Ministry of Education of China (20100161110011), Hunan Provincial Natural Science Foundation (Grant 11JJ1002), and the National Natural Science Foundation of China (21072052).

References

[1] Assaf SY, Chung SH. Release of endogenous Zn^{2+} from brain tissue during activity. *Nature* 1984;308:734.

[2] O'Halloran TV. Transition metals in control of gene expression. *Science* 1993; 261:715.

[3] Berg JM, Shi YG. The galvanization of biology: a growing appreciation for the roles of zinc. *Science* 1996;271:1081.

[4] Frederickson CJ, Hernandez MD, McGinty JF. Translocation of zinc may contribute to seizure-induced death of neurons. *Brain Res* 1989;480:317.

[5] Bush A, Pettingell W, Multhaup G, Paradis M, Vonsattel J, Gusella J, et al. Rapid induction of Alzheimer A beta amyloid formation by zinc. *Science* 1994;265: 1464.

[6] Zeeb M, Sadeghi M. Modified ionic liquid cold-induced aggregation dispersive liquid–liquid microextraction followed by atomic absorption spectrometry for trace determination of zinc in water and food samples. *Microchim Acta* 2011;175:159.

[7] Silvestre MD, Lagarda MJ, Farre R, Martinez-Costa C, Brines J. Copper, iron and zinc determinations in human milk using FAAS with microwave digestion. *Food Chem* 2000;68:95.

[8] Panayi AE, Spyrou NM, Iversen BS, White MA, Part P. Determination of cadmium and zinc in Alzheimer's brain tissue using Inductively Coupled Plasma Mass Spectrometry. *J Neuro Sci* 2002;195:1.

[9] Boevski IV, Daskalova N, Havezov I. Determination of barium, chromium, cadmium, manganese, lead and zinc in atmospheric particulate matter by inductively coupled plasma atomic emission spectrometry (ICP-AES). *Spectrochim Acta B* 2000;55:1643.

[10] Weber G, Alt F, Messerschmidt J. Characterization of low-molecular-weight metal species in plant extracts by using HPLC with pulsed amperometric detection and cyclic voltammetry. *Fresenius J Anal Chem* 1998;362:209.

[11] Wong BA, Friedle S, Lippard SJ. Solution and fluorescence properties of symmetric dipicolylamine-containing dichlorofluorescein-based Zn^{2+} sensors. *J Am Chem Soc* 2009;131:7142.

[12] Buccella D, Horowitz JA, Lippard SJ. Understanding zinc quantification with existing and advanced ditopic fluorescent zinypr sensors. *J Am Chem Soc* 2011;133:4101.

[13] Lu XY, Zhu WH, Xie YS, Li X, Gao Y, Li FY, et al. Near-IR core-substituted naphthalenediimide fluorescent chemosensors for zinc ions: ligand effects on PET and ICT channels. *Chem Eur J* 2010;16:8355.

[14] Tang B, Huang H, Xu K, Tong L, Yang G, Liu X, et al. Highly sensitive and selective near-infrared fluorescent probe for zinc and its application to macrophage cells. *Chem Commun* 2006:3609.

[15] Grabowski ZR, Rotkiewicz K, Rettig W. Structural changes accompanying intramolecular electron transfer: focus on twisted intramolecular charge-transfer states and structures. *Chem Rev* 2003;103:3899.

[16] Komatsu K, Urano Y, Kojima H, Nagano T. Development of an Iminocoumarin-based zinc sensor suitable for ratiometric fluorescence imaging of neuronal zinc. *J Am Chem Soc* 2007;129:13447.

[17] Zhang Y, Guo X, Si W, Jia L, Qian X. Ratiometric and water-soluble fluorescent zinc sensor of carboxamidoquinoline with an alkoxyethylamino chain as receptor. *Org Lett* 2008;10:473.

[18] van Dongen EMWM, Dekkers LM, Spijker K, Meijer EW, Klomp LWJ, Merckx M. Ratiometric fluorescent sensor proteins with subnanomolar affinity for $\text{Zn}(\text{II})$ based on copper chaperone domains. *J Am Chem Soc* 2006;128:10754.

[19] van Dongen EMWM, Evers TH, Dekkers LM, Meijer EW, Klomp LWJ, Merckx M. Variation of linker length in ratiometric fluorescent sensor proteins allows rational tuning of $\text{Zn}(\text{II})$ affinity in the picomolar to femtomolar range. *J Am Chem Soc* 2007;129:494.

[20] Han ZX, Zhang XB, Li Z, Gong YJ, Wu XY, Jin Z, et al. Efficient fluorescence resonance energy transfer-based ratiometric fluorescent cellular imaging probe for Zn^{2+} using a rhodamine spirolactam as a trigger. *Anal Chem* 2010; 82:3108.

[21] Weng Y, Chen ZL, Wang F, Xue L, Jiang H. High sensitive determination of zinc with novel water-soluble small molecular fluorescent sensor. *Anal Chim Acta* 2009;647:215.

[22] Xu Z, Baek KH, Kim HN, Cui J, Qian X, Spring DR, et al. Zn^{2+} -triggered amide tautomerization produces a highly Zn^{2+} -selective, cell-permeable, and ratiometric fluorescent sensor. *J Am Chem Soc* 2009;132:601.

[23] Wang B, Wang YC, Hua JL, Jiang YH, Huang JH, Qian SX, et al. Starburst triarylamine donor–acceptor–donor quadrupolar derivatives based on cyano-substituted diphenylaminestyrylbenzene: tunable aggregation-induced emission colors and large two-photon absorption cross sections. *Chem Eur J* 2011;17:2647.

[24] Sun F, Zhang GX, Zhang DQ, Xue L, Jiang H. Aqueous fluorescence turn-on sensor for Zn^{2+} with a tetraphenylethylene compound. *Org Lett* 2011;13: 6378.

[25] Yin SC, Zhang J, Feng HK, Zhao ZJ, Xu LW, Qiu HY, et al. Zn^{2+} -selective fluorescent turn-on chemosensor based on terpyridine-substituted siloles. *Dyes Pigments* 2012;95:174.

[26] Măluțan T, Măluțan APC, Tătaru L, Humelnicu D. A fluorescence emission, FT-IR and UV–VIS absorption study of the some uranium (VI) Schiff bases complexes. *J Fluoresc* 2008;18:707.

[27] Tang WX, Xiang Y, Tong AJ. Salicylaldehyde azines as fluorophores of aggregation-induced emission enhancement characteristics. *J Org Chem* 2009; 74:2163.

[28] Salavati-Niasari M, Amiri A. Synthesis and characterization of alumina-supported $\text{Mn}(\text{II})$, $\text{Co}(\text{II})$, $\text{Ni}(\text{II})$ and $\text{Cu}(\text{II})$ complexes of bis(salicylaldiminato) hydrazone as catalysts for oxidation of cyclohexene with tert-buthylhydroperoxide. *Appl Catal A Gen* 2005;290:46.